

# Plasma Spray Coatings of Ni-Al-SiC Composite

S.M. Hashemi, M.H. Enayati, and M.H. Fathi

(Submitted October 17, 2008; in revised form December 1, 2008)

Ni-Al-SiC powder mixture containing 12 wt.% SiC was prepared by conventional ball milling. Morphological and microstructural investigations showed that powder particles after 15 h of milling time had the optimum characteristics with respect to their size and microstructure. X-ray diffraction patterns of powder particles included only the elemental Ni, Al, and SiC peaks without any traces of oxides or intermetallic phases. The powder mixture was then deposited onto a steel substrate by atmospheric plasma spray (APS) process under different conditions. The results showed that under APS conditions used here, the coatings were composed of various intermetallics including Ni-Al and Ni<sub>2</sub>Al<sub>3</sub>. The mean hardness of coating was found to be about 567 HV. It was also found that by increasing current density of APS, the coating/substrate adhesive strength was increased.

**Keywords** adhesion test, ball milling, composite, hardness, nickel aluminide, plasma spray

## 1. Introduction

Many intermetallic compounds (ICs), including nickel aluminides, display an attractive combination of physical and mechanical properties including high melting temperature, high hardness, low density, and good oxidation and corrosion resistance (Ref 1-7), which make them suitable materials for structural applications especially at high temperatures such as gas turbine, automobile engine, aircraft, and heat treatment fixtures (Ref 5-9). Research on nickel aluminides has been expanded during the last 30 years, not only as bulk materials, but also as coatings (Ref 10-12). Studies have indicated that nickel aluminide alloys have significant potential in wear applications as wear properties of carbon steel parts can be significantly improved by applying nickel aluminide coating (Ref 12, 13).

Plasma spraying is the most flexible/versatile thermal spray process with respect to the sprayed materials. The high temperatures of plasma spraying permit the deposition of coatings for application in areas of liquid and high-temperature corrosion and wear protection and also special application for thermal, electrical, and biomedical purposes. As a result of the nickel-aluminum (Ni-Al) exothermic reaction, partial fusion/welding between coating and substrate occurs, improving the bond strength. This is the main reason for applying Ni-Al materials as

bond coatings (Ref 10, 11, 14, 15). Different results are available concerning the completeness of the Ni-Al reaction during the spraying and the type of aluminide formed (Ref 11). Phase composition in coatings sprayed using Ni-Al powders of different compositions by atmospheric plasma spray (APS) method was studied by Sampath et al. (Ref 16). They reported that the APS coatings contain Ni and Al oxides or contain Al<sub>2</sub>O<sub>3</sub> together with a solid solution of Al in Ni ( $\alpha$ Ni). The chemical reaction between different elements occurs during particle flight in the APS flame. The molten Ni and Al form intermetallic compounds in the presence of oxides (Ref 17-19).

Mechanical milling has recently been developed as one of the techniques to prepare composite powders mechanically by ball milling different kinds of powders. A rigid bond between the particles is created by cold welding when mechanical energy is applied to powder particles (Ref 20). Such binderless composite powders can be thermally sprayed to form coatings on various substrates (Ref 21-24).

Incorporation of hard second phases into an IC matrix is a strategy for effective high-temperature strengthening, creating an intermetallic matrix composite (IMC). Recently, a great deal of work has been done on intermetallic matrix composites (IMCs). Various continuous or discontinuous ceramic reinforcements such as SiC, Al<sub>2</sub>O<sub>3</sub>, TiB<sub>2</sub>, and TiC were explored to obtain increased high-temperature strength and better creep resistance, together with adequate ductility and toughness (Ref 25-29). Among these reinforcements, SiC fibers were commercialized for use in IMCs (Ref 30-32). In the previous studies, the SiC reinforcements were added into different nickel aluminide matrices by reaction synthesis (Ref 30), mechanically alloying (Ref 31), and sintering (powder metallurgy) (Ref 32) to improve oxidation and mechanical properties and the workability of the matrices. In the present study, nickel aluminide matrix composite coating reinforced by SiC particulates was fabricated by the APS of Ni-Al-SiC

S.M. Hashemi, M.H. Enayati, and M.H. Fathi, Department of Materials Engineering, Isfahan University of Technology (IUT), Isfahan 84156-83111, Iran. Contact e-mail: ma\_hashemi@alumni.iut.ac.ir.

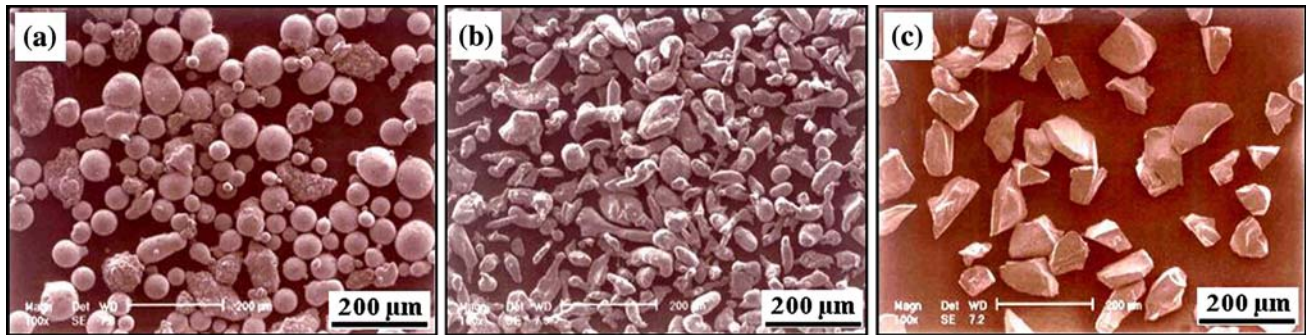


**Fig. 1** SEM images of as-received powder particles. (a) Ni. (b) Al. (c) SiC

**Table 1** APS parameters

Feedstock type	Metallization PS50M
Current, A	600, 700, 800
Voltage, V	28
Plasma gas	Ar
Ar pressure, kPa	500
Jet gun	6 mm external
Carrier pressure, kPa	30
Feed rate, g/min	30
Spray distance, mm	100, 125, 150
Torch transfer speed, mm/s	30
Substrate thickness, mm	9
Number of pass	2

powder prepared by ball milling. The structural evolutions and characteristics of powder particles and the prepared plasma sprayed coatings are investigated in detail.

## 2. Experimental Procedure

### 2.1 Feedstock Preparation

The raw powders of Ni (30-70  $\mu\text{m}$ , 98% purity) and Al (45-65  $\mu\text{m}$ , 98% purity) with composition of  $\text{Ni}_{75}\text{Al}_{25}$  (at.%) were ball milled with 12 wt.% SiC (100-140  $\mu\text{m}$ ) as reinforcement particles by a conventional tumbler ball mill using hardened steel jar and balls. Morphology of the initial powder particles is given in Fig. 1. Ball milling was carried out at room temperature under Ar atmosphere and at a rotating speed of 85 rpm with ball-to-powder ratio of 20:1. Samples were taken at selected time intervals of milling for further examination.

### 2.2 Plasma Spraying

Atmospheric plasma spraying was carried out using a Metallization PS50M plasma spray system (Poodr Afshan Company (PACO), Isfahan Science and Technology Town, Isfahan, Iran) with conditions listed in Table 1.

The CK45 steel substrates, with composition shown in Table 2, were cut into pieces of 90 by 9 by 9 mm dimensions, mechanically ground, and then polished. Prior to spraying, the samples were sandblasted by SiC particles (0.2-0.5 mm).

The powder was milled for 15 h and then deposited onto substrates at different spray distances and current intensities (Table 3).

### 2.3 Characterization

Microstructure and morphology of powder particles and as-sprayed coatings were investigated using a Philips XL30 scanning electron microscope (SEM) (SEM laboratory of materials engineering department, Isfahan University of Technology, Isfahan, Iran) equipped with an energy-dispersive x-ray analyzer (EDAX). Phase compositions of the powders and coatings were carefully analyzed by x-ray diffraction (XRD) in a Philips X'PERT MPD diffractometer (SEM laboratory of materials engineering department, Isfahan University of Technology, Isfahan, Iran) using filtered  $\text{Cu K}\alpha$  radiation ( $\lambda = 0.1542 \text{ nm}$ ). The goniometer was set at a scan rate of  $0.05^\circ/\text{s}$  over a  $2\theta$  range of  $20^\circ$  to  $100^\circ$ .

A Vickers indenter was used to measure the microhardness of coatings at a load of 0.98 N. The macrohardness of coatings was also measured at a load of 5 kg. Each hardness value was the average of 10 measurements.

An interfacial indentation test is often used as an alternative to other tests in terms of apparent interface toughness (Ref 33). The interfacial indentation test consists of measuring the length of a crack generated at the coating/substrate interface as a result of a Vickers indentation at the interface using different applied loads (Fig. 2).

In bilogarithmic coordinates, the relation between the crack length and the applied load is linear and allows defining a critical load under which no crack is generated at the interface (Ref 33, 34).

For adhesion determination using Vickers, five indentations were performed for each level of load to determine a reliable mean crack length.

## 3. Results and Discussion

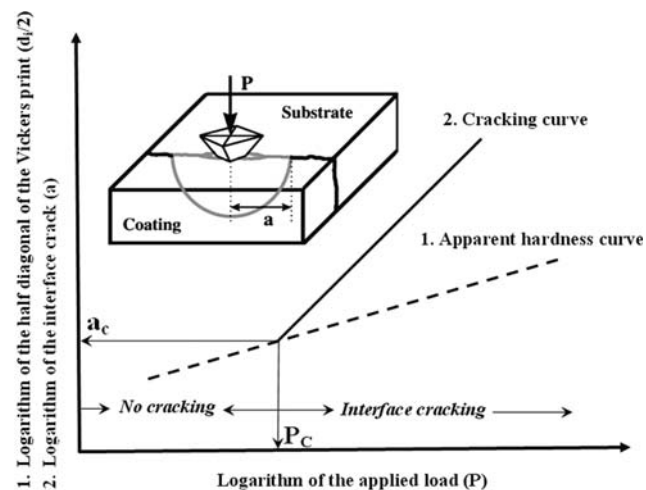
Figure 3 shows scanning electron micrographs of the  $\text{Ni}_{75}\text{Al}_{25}$ -12 wt.%SiC powder particles after 5, 10, 15, and 20 h of ball milling. Figure 4 shows the variation of mean powder particle size after different milling times. As

**Table 2** Nominal composition of CK45 steel substrate

Composition, wt. %											
Fe	C	Si	P	S	Mn	Ni	Cr	Mo	Cu	Al	V
98.46	0.444	0.280	0.099	0.0167	0.702	<0.030	0.010	0.0185	0.0237	0.0125	0.0030

**Table 3** APS conditions

Condition code	C1	C2	C3	C4	C5
Spray distance, mm	100	125	150	125	125
Spray current intensity, A	600	600	600	700	800

**Fig. 2** Principle of interface indentation test and schematic representation of results

shown, after milling for 5 h, Ni and Al powder particles were only mixed and had no deformed characteristics. After longer milling times (10, 15, and 20 h), however, the powder particles were extensively deformed. As a result of low energy of milling and the existence of brittle SiC powder, the size of the powder particles continuously reduced (Fig. 4), and their size distribution and morphology became more uniform by increasing the milling time. After 20 h of milling, the mean powder particle size was about 40  $\mu\text{m}$ . The milling process stopped at this stage, because longer milling time led to finer powder particles that are unsuitable for thermal spraying. A fine particle size causes several problems in APS, including nonuniformity in the powder feed rate and a decrease in powder flux, therefore increasing porosity and decreasing adherence and quality of coatings (Ref 35). It was found that the powder particles milled for 15 h had suitable size (46  $\mu\text{m}$ ) for thermal spraying.

The cross-sectional SEM images of the powder particles after different milling times are presented in Fig. 5. In the early stage of milling, the Ni and Al phases were deformed and extensively cold welded, forming a metal/metal composite structure (Fig. 5a, b). At this stage, only a small fraction of fractured SiC particles were incorporated into the powder particles. On further milling, the Al/Ni

irregular structure became finer and more SiC particles were incorporated into the Al/Ni powder particles as shown in Fig. 5(c) and (d). Simultaneously, SiC particles fractured extensively and their average size reduced significantly.

Figure 6 shows XRD patterns of the Ni<sub>75</sub>Al<sub>25</sub>-12 wt.%SiC composite powders after different milling times. As shown, the sharp crystalline diffraction peak of initial powders progressively broadened with increasing milling time associated with accumulated internal strain and refinement of grain size as a result of plastic deformations and work hardening of powder particles during ball milling (Ref 36). No new phase including Ni-Al solid solution or intermetallics was formed during ball milling. In contrast, Enayati et al. (Ref 37) reported that ball milling of Ni<sub>75</sub>Al<sub>25</sub> powder mixture in a high-energy ball mill (planetary type), led to the formation of a Ni(Al) solid solution that transformed to nickel aluminide on further milling. The extent of plastic deformation of powder particles, the local increase of temperature, and also the increase in the density of lattice defects in low-energy ball mills (i.e., tumbler) and therefore the mass transport by diffusion are smaller compared to those in high-energy ball mills (i.e., planetary ball mills), making it impossible to obtain nickel aluminide phase (Ref 23, 38). In fact, the lack of formation of nickel aluminide compound during milling is beneficial as an exothermic reaction between Ni-Al occurs during thermal spraying, improving the adhesive strength of coatings.

The formation of Ni-Al intermetallic compounds required a long time and a high temperature for the diffusion of Al and Ni. In thermal spray processes, the temperature is high enough for diffusion, but the exposure time of powders to plasma flame is too short. On the other hand, in the plasma spray process, melted particles are solidified with a very high rate (10<sup>6</sup>/s to 10<sup>8</sup>/s). After powder deposition on the substrate, the high-temperature diffusion and therefore the Ni-Al reaction is stopped (Ref 10, 39). It should be noted that by increasing the spray distance the diffusion time increased, while by increasing current density of APS the plasma flame temperature increased. These two parameters determine the content of intermetallic compound in the coatings.

The XRD patterns of APS coatings prepared at different conditions are shown in Fig. 7. In all traces the relative intensity of Ni<sub>2</sub>Al<sub>3</sub> peaks was low. This shows that there was not enough time for a Ni-Al reaction during APS. Also it was observed that by increasing the current intensity from 600 to 700 A, the relative intensity of Ni decreased while that of Ni<sub>2</sub>Al<sub>3</sub> phase increased, whereas by increasing the current intensity from 700 to 800 A, a reverse trend was observed. As the current intensity

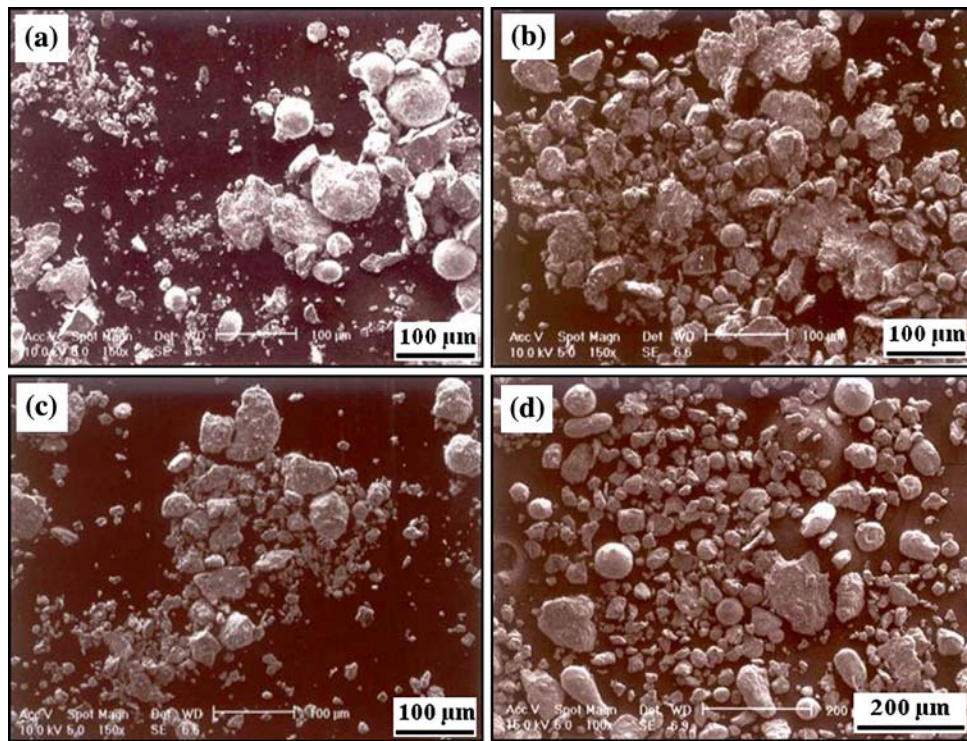


**Fig. 3** Scanning electron micrographs of the Ni-Al-SiC powder particles after different milling times. (a) 5 h. (b) 10 h. (c) 15 h. (d) 20 h

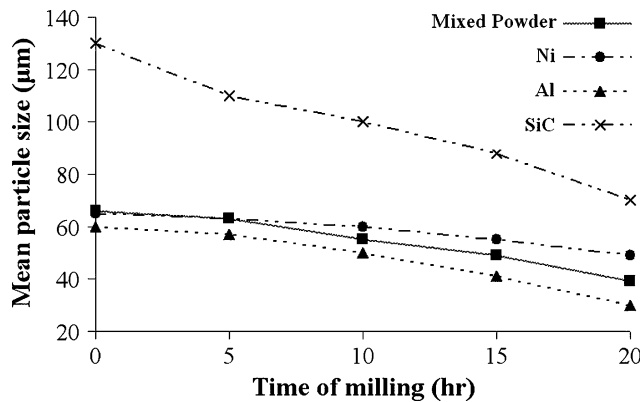


**Fig. 4** Variation of mean powder particle size versus milling time

increases, the temperature distribution of flame is disturbed and the powder particles are passed in lower-temperature regions of the flame or are passed for a shorter time through the higher-temperature regions (Ref 40). On the other hand, the increased current density will increase the velocity of the flow rate of the powder spray, thus increasing the dwelling time of the powder particles and further decreasing the XRD intensity of  $\text{Ni}_2\text{Al}_3$  peaks. In fact, the dwelling time of the particles inside the flame is also important. In this case, powder particles experience lower heat, which eliminates the diffusion of Ni and Al and therefore the development of Ni-Al compounds.

According to the Ni-Al phase diagram, Ni and Al can make various intermetallic compounds including  $\text{NiAl}_3$ ,

$\text{Ni}_2\text{Al}_3$ ,  $\text{NiAl}$ ,  $\text{Ni}_5\text{Al}_3$ , and  $\text{Ni}_3\text{Al}$ . The free energy of formation ( $\Delta G$ ) of  $\text{Ni}_2\text{Al}_3$  phase up to 1000 °C is smaller compared to the other compounds. Therefore, during APS  $\text{Ni}_2\text{Al}_3$  phase is expected to favorably form (Ref 10). Also, NiAl compound has a very broad range of composition in the phase diagram and can be obtained in different ratios of nickel and aluminum. Thus, formation of NiAl and  $\text{Ni}_2\text{Al}_3$  phases in Ni-Al plasma sprayed coatings is preferred. On the other hand, low-energy ball milling does not generate enough energy to make a thin alternative layer of elemental powders. Therefore, some elemental Ni can remain in the APS coating. This is the reason for changes in ratio of nickel and aluminum in some regions that forms different Ni-Al intermetallic phases.

It was found that by increasing spray distance, the content of intermetallic compounds in the coating was increased as a result of an increase in Ni-Al diffusion time. On other hand, it was observed that deposition efficiency of powders on the substrate in the C2 condition was greater than in the C3 condition. Consequently, 125 mm was selected as the optimum spray distance. Thus, plasma spraying was carried out at 125 mm spray distance and higher current densities (conditions C4, C5). By increasing the current density of the thermal spray process, the plasma flame temperature increases and then the porosity content of coatings decreases, as a result of more complete melting and therefore better seating of powder particles beside each other. The cross-sectional microstructure of as-sprayed coating in the C4 condition (optimum spray condition) is shown in Fig. 8. Such layer coating microstructures were obtained in any conditions.

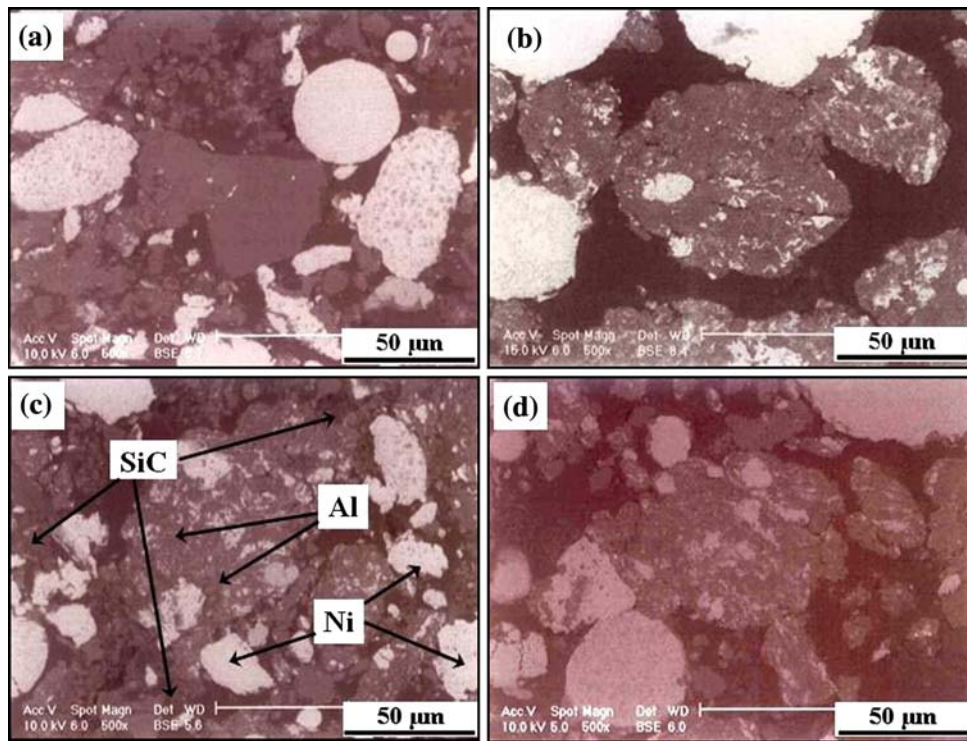


**Fig. 5** Cross-sectional SEM images of Ni-Al-SiC powder particles after different milling times. (a) 5 h. (b) 10 h. (c) 15 h. (d) 20 h

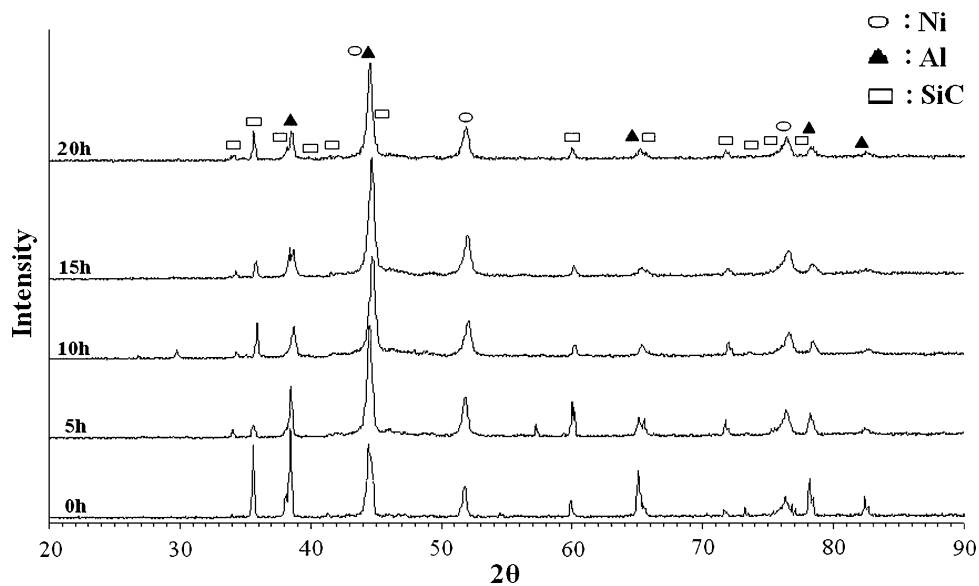


**Fig. 6** XRD patterns of Ni-Al-SiC composite powders after different milling times

The microhardnesses of versatile phases of coating are listed in Table 4. Different phases in microstructure were identified by EDAX and XRD patterns. Large phase “a” with a mean hardness of 246 HV was identified as Ni; the work-hardening effect during ball milling and impact of powder particles onto the substrate during APS is the cause of its high hardness.

Phase “b” had a mean hardness of 518 HV and was identified as a NiAl phase. As pointed out previously, the NiAl phase is a large solubility phase in the Ni-Al phase diagram. Depending on the content of Ni and Al, the hardness of NiAl can be different. Gray phase “c” has a high hardness about 538 HV. EDAX analysis revealed that this phase is Ni<sub>2</sub>Al<sub>3</sub> phase. Dark phase “d” with a

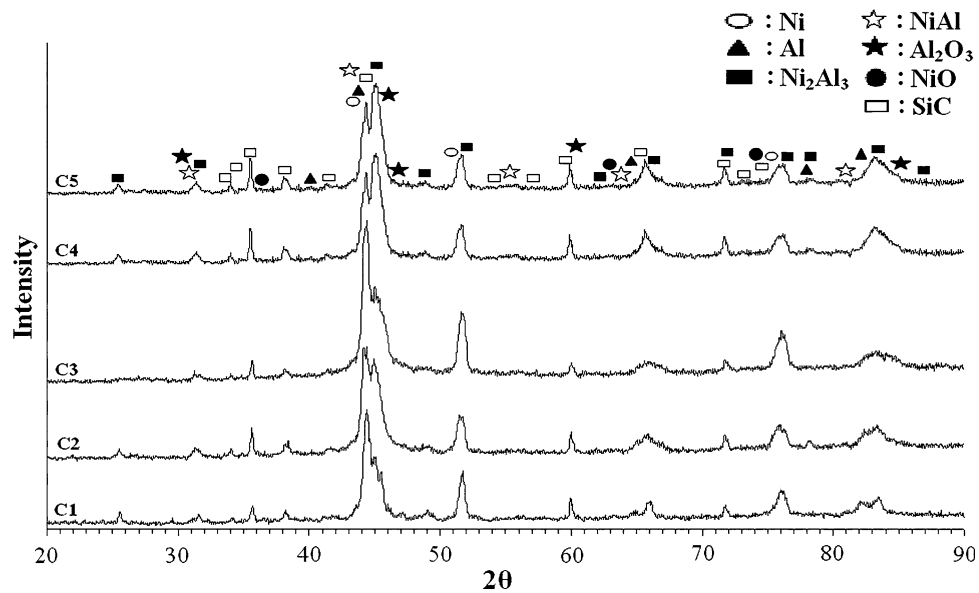


Fig. 7 XRD patterns of as-sprayed coatings prepared at different conditions

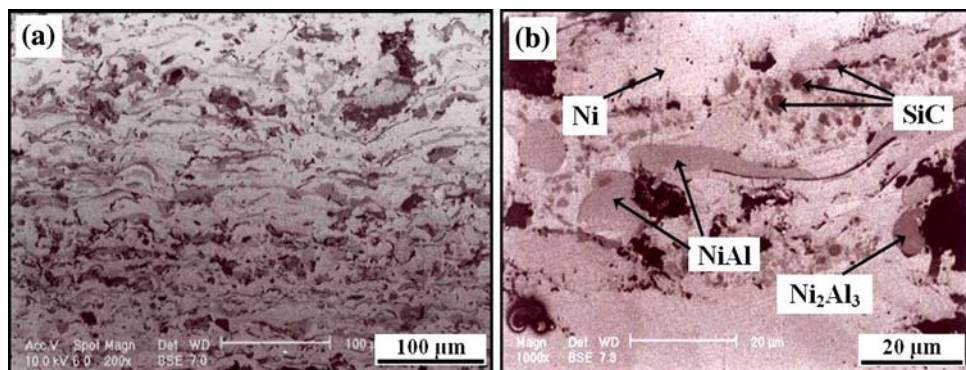


Fig. 8 Cross-sectional SEM images of coating deposited at C4 condition. (b) Higher magnification than (a)

Table 4 Vickers microhardness of various phases in the coatings

Phase	a	b	c	d
Microhardness, HV				
Max	286	572	882	904
Min	206	464	824	888
Mean	246 ± 40	518 ± 54	853 ± 29	901 ± 3

hardness of 901 HV was SiC particles. The macrohardness value of APS coatings was also measured at 567 HV.

Interfacial indentation tests were carried out on APS coatings using Vickers microhardness under loads of 0.98, 1.96, 2.94, and 4.9 N for adhesion strength examination of coatings. Figure 9 shows cross-sectional SEM micrographs of the coating/substrate interface. By increasing loads of indenter and at a load of 4.9 N, cracks with length of about 45 μm were created in the coating/substrate interface of samples sprayed in the C2 and C4 conditions, while no

crack occurred in the C5 condition. By increasing current densities, both spray temperature and coating density were increased. As a result, those coatings that were sprayed at higher current densities exhibited higher adhesive strength.

#### 4. Conclusions

Ni-Al-SiC composite powder containing 12 wt.% SiC was prepared by ball milling in a conventional tumbler mill. The Ni-Al-SiC powder was then sprayed onto a carbon steel substrate by atmospheric plasma spraying to obtain a nickel-aluminide/SiC composite coating. The results showed that spray distance and current intensity of spraying have a significant influence on the phase composition of the coatings, the plasma spray efficiency, and the mechanical properties of coatings.

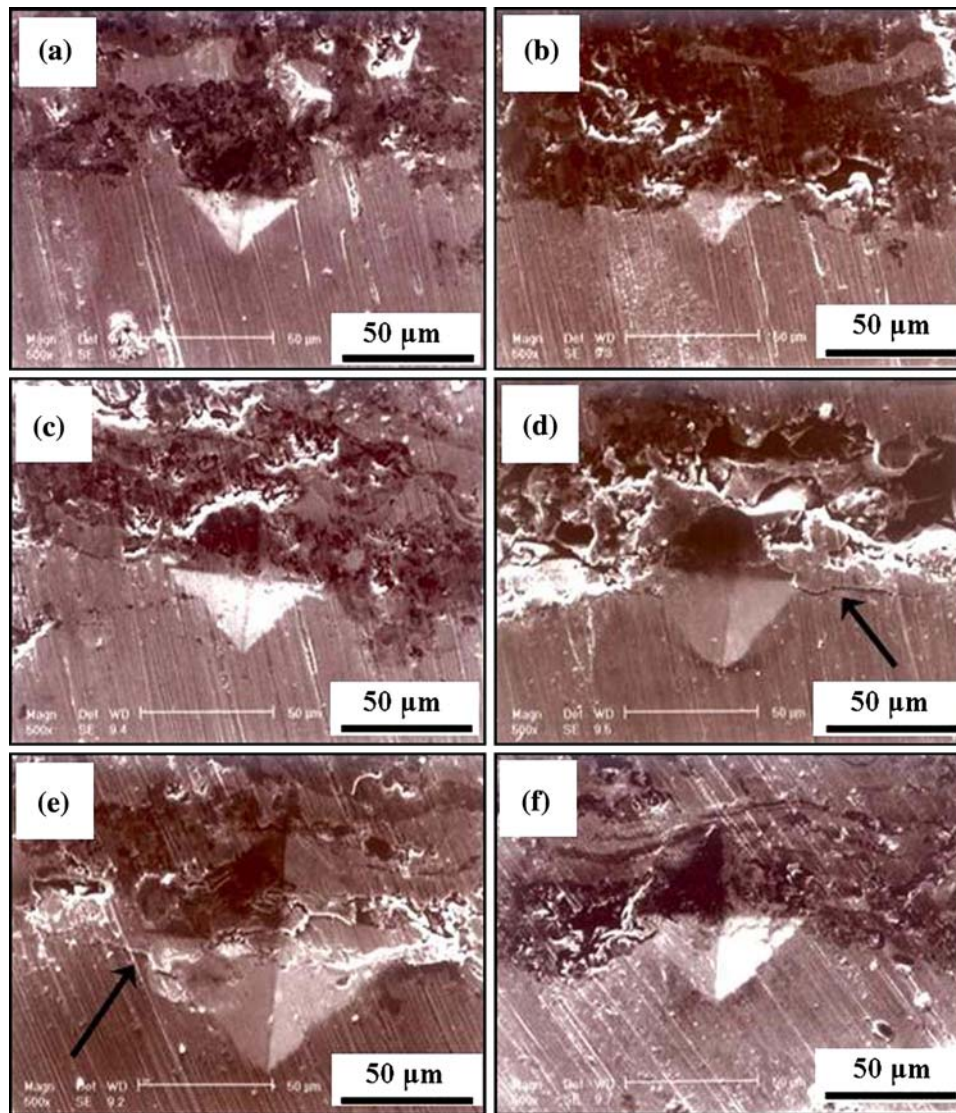


**Fig. 9** Interfacial indentation test under different conditions and loads. (a) C2, 0.98 N. (b) C2, 1.96 N. (c) C2, 2.94 N. (d) C2, 4.9 N. (e) C4, 4.9 N. (f) C5, 4.9 N

Microstructural studies as well as hardness tests showed that the coatings consisted of NiAl and Ni<sub>2</sub>Al<sub>3</sub> intermetallic phases along with αNi solid solution and SiC reinforcement.

The mean hardness of coatings was measured to be about 567 HV. The adhesion test showed that the plasma sprayed coatings had high adhesive coating/substrate strength that was increased by increasing the spray current intensity.

### Acknowledgment

The authors acknowledge the Poodr Afshan Company (PACO) in Isfahan Science and Technology Town, for providing APS equipments.

### References

1. G. Sauthoff, *Intermetallics*, Chap. 2, 4, Weinheim, New York, 1995
2. J.H. Westbrook and R.L. Fleischer, *Intermetallic Compounds*, Chap. 27, 30, Vol. 3, John Wiley & Sons, New York, 2002
3. J.K. Tien and T. Caulfield, *Superalloys, Supercomposite and Superceramics*, Chap. 18, Harcourt Brace Jovanovich, New York, 1989
4. T. Czeppe and S. Wierzbinski, Structure and Mechanical Properties of NiAl and Ni<sub>3</sub>Al Based Alloys, *Int. J. Mech. Sci.*, 2000, **42**, p 1499
5. J.H. Westbrook and R.L. Fleischer, *Intermetallic Compounds*, Chap. 1-3, Vol. 2, John Wiley & Sons, New York, 1994
6. N.S. Stoloff, Physical and Mechanical Metallurgy of Ni<sub>3</sub>Al and Its Alloys, *Int. Mater. Rev.*, 1989, **34**(4), p 153-160
7. *ASM Specialty Handbook: Nickel, Cobalt, and Their Alloys*, J.R. Davis, Ed., ASM International, Materials Park, OH, 2000
8. C.C. Berndt, Thermally Sprayed Coatings: Properties and Applications, *Proc. Fourth International Conference* (Paris, France), ASM International, 1990, p 193-200

9. N.S. Stoloff, C. T. Liu, and S.C. Deevi, Emerging Applications of Intermetallics, *Intermetallics*, 2000, **8**, p 1313
10. J.M. Houben and J.H. Zaat, Investigations into the Mechanism of Exothermically Reacting Nickel-Aluminum Spraying Materials, *Proc. Seventh International Metal Spray Conference* (London), Sept 1973, Welding Institute, p 77-88
11. O. Knotek, E. Lugscheider, and H.R. Eschnauer, Reactive Kinetic Observations for Spraying with Ni-Al Powder, *Proc. Seventh International Metal Spray Conference* (London), Sept 1973, Welding Institute, p 72-76
12. D.S. Rickerby and A. Matthews, *Advanced Surface Coatings: A Handbook of Surface Engineering*, Chapman and Hall, New York, 1991
13. H. Goldenstein, Y.N. Silva, and H.N. Yoshimura, Designing a New Family of High Temperature Wear Resistant Alloys Based on Ni<sub>3</sub>Al IC: Experimental Results and Thermodynamic Modeling, *Intermetallics*, 2004, **12**, p 963
14. S.C. Deevi, V.K. Sikka, C.J. Swindeman, and R.D. Seals, Reactive Spraying of Nickel-Aluminide Coatings, *J. Therm. Spray Technol.*, 1997, **6**, p 335
15. M. Evrard and V. Vesely, Consumables, *Seventh International Metal Spraying Conference*, Vol 2, 1973, p 289-295
16. S. Sampath, B. Gudmundsson, R. Tiwari, and H. Herman, Plasma Spray Consolidation of Ni-Al Intermetallics, *Proc. Third National Thermal Spray Conference* (Long Beach, CA), May 1990, ASM International, p 357
17. C.Y. Chung, M. Zhu, and C.H. Man, Effect of Mechanical Alloying on the Solid State Reaction Processing of Ni-36.5 at.% Al Alloy, *Intermetallics*, 2002, **10**, p 865
18. M.L. Allan, D. Otterson, and C.C. Berndt, *Plasma Sprayed Ni-Al Coatings for Safe Ending Heat Exchanger Tubes*, BNL Report, Brookhaven National Laboratory, Upton, NY, 1998
19. J.A. Hearley, J.A. Little, and A.J. Sturgeon, The Effect of Spray Parameters on the Properties of High Velocity Oxy-Fuel NiAl Intermetallic Coatings, *Surf. Coat. Technol.*, 2000, **123**, p 210
20. T. Chen, J.M. Hampikian, and N.N. Thadhani, Synthesis and Characterization of Mechanically Alloyed and Shock-Consolidated Nanocrystalline NiAl Intermetallic, *Acta Mater.*, 1999, **8**, p 2567
21. S. Rangaswamy, US Patent No. 5631044
22. C. Suryanarayana, Mechanical Alloying and Milling, *Prog. Mater. Sci.*, 2001, **46**, p 1
23. M.S. El-Eskandarany, *Mechanical Alloying for Fabrication of Advanced Engineering Materials*, Chap. 1, Noyes Publications, 2001, New York, p 1-21, 2001
24. R. Maric, K.N. Ishihara, and P.H. Shingu, Structural Changes During Low Energy Ball Milling in the Ni-Al System, *J. Mater. Sci. Lett.*, 1996, **15**, p 1180
25. J.H. Yi and C.C. Berndt, An Electron Microscopic Examination of Composite Coatings Produced by Thermal Spraying, *Surface Modification Technology*, 1991, **4**, p 299-310
26. P. Becher and K. Plucknett, Properties of Ni<sub>3</sub>Al Bonded Titanium Carbide Ceramics, *J. Euro. Ceram. Soc.*, 1997, **18**, p 395
27. M. Inoue, K. Suganuma, and K. Nihara, Fracture Mechanism of Ni<sub>3</sub>Al Alloys and their Composites with Ceramic Particle at Elevated Temperatures, *Intermetallics*, 2000, **8**, p 365
28. M. Inoue, K. Takahashi, and K. Nihara, Effects of Boron Doping on Fracture Properties of Ni<sub>3</sub>Al Matrix Composites with Ceramic Particles, *Scr. Mater.*, 1998, **39**, p 887
29. Y. Wujun, F. Di, and L. Heli, The Microstructure and Its Properties of Ni<sub>3</sub>Al Based Composite, *Mater. Res. Innov.*, 1999, **2**, p 321
30. L. Plazanet, D. Tetard, and F. Nardou, Effect of SiC and ZrO<sub>2</sub> Particles on the Mechanical Properties of NiAl, *Compos. Sci. Technol.*, 1999, **59**, p 537
31. D.L. Zhang, J. Liang, and J. Wu, Processing Ti<sub>3</sub>Al-SiC Nanocomposites High Energy Mechanical Milling, *Mater. Sci. Eng.*, 2004, **A375**, p 911
32. D.B. Lee and D. Kim, The Oxidation of Ni<sub>3</sub>Al Containing Decomposed SiC Particles, *Intermetallics*, 2001, **9**, p 51
33. G. Marot, J. Lesage, Ph Demarecaux, M. Hadad, St Sieymann, and M.H. Staia, Interfacial Indentation and Shear Tests to Determine the Adhesion of Thermal Spray Coatings, *Surf. Coat. Technol.*, 2006, **201**, p 2080
34. P. Araujo, D. Chicot, M. Staia, and J. Lesage, Residual Stress and Adhesion of Thermal Spray Coatings, *Surf. Eng.*, 2005, **21**, p 35
35. M.A. Clegg, V. Aim, and D.J. Silins, Composite Powder in Thermal Spray Applications, *Seventh International Metal Spray Conference* (London), The Welding Institute, 1973, p 62-71
36. B.D. Cullity, *Elements of X-ray Diffraction*, Addison-Wesley, Reading, MA, 1978
37. M.H. Enayati, Z. Sadeghian, M. Salehi, and A. Saidi, The Effect of Milling Parameters on the Synthesis of Ni<sub>3</sub>Al Intermetallic Compound by Mechanical Alloying, *Mater. Sci. Eng.*, 2004, **A375-377**, p 809
38. V.V. Boldyrev and K. Tkacova, Mechanochemistry of Solids: Past, Present and Prospects, *J. Mater. Syn. Process*, 2000, **8**, p 121
39. S. Sampath, X.Y. Jiang, and J. Matejicek, Role of Thermal Spray Processing Method on the Microstructure, Residual Stress and Properties of Coatings: an Integrated Study for Ni-5wt.%Al Bond Coats, *Mater. Sci. Eng.*, 2004, **A236**, p 216
40. R.F. Bunshah, *Handbook of Hard Coatings*, William Andrew, Norwich, NY, 2003